

Efficient diagnostics for quantum error correction

Pavithran Iyer,^{1,2,3} Aditya Jain,^{1,2,3,4} Stephen D. Bartlett,⁵ and Joseph Emerson^{1,2,3,4}

¹*Department of Applied Mathematics, University of Waterloo, Waterloo, Ontario N2L 3G1, Canada.*

²*Institute for quantum computing, University of Waterloo, Waterloo, Ontario N2L 3G1, Canada.*

³*Quantum Benchmark Inc., Kitchener, Ontario N2H 5G5, Canada.*

⁴*Keysight Technologies Canada, Kanata, ON K2K 2W5, Canada.*

⁵*Centre for Engineered Quantum Systems, School of Physics, University of Sydney, Sydney, New South Wales 2006, Australia.*

Fault-tolerant quantum computing will require accurate estimates of the resource overhead, but standard metrics such as gate fidelity and diamond distance have been shown to be poor predictors of logical performance. We present a scalable experimental approach based on Pauli error reconstruction to predict the performance of concatenated codes. Numerical evidence demonstrates that our method significantly outperforms predictions based on standard error metrics for various error models, even with limited data. We illustrate how this method assists in the selection of error correction schemes.

Noise is pervasive in quantum processing, and must be overcome to achieve the disruptive capabilities of quantum computing. Fault tolerance guarantees reliable logical quantum computation in the presence of noise under prescribed conditions often oversimplified as achieving a threshold on gate error rates. However, achieving low logical error rates in practice is a significant challenge, in part because of the large overheads that are required in terms of the number of additional qubits and gates. The design and selection of an error correction strategy for a particular platform requires accurate prediction of its expected logical performance. For instance, in the presence of biased noise [1–6], tailored codes have been shown to outperform traditional codes that are designed to correct unstructured noise. However, bias is only one of the exponentially many parameters that describe the noise on n physical qubits. This work addresses the lack of tools for predicting the logical performance of a FT architecture based on a description of noise at the physical level.

The existing theoretical framework for choosing a FT scheme is centered around the fault tolerance accuracy threshold theorem [7, 8] which provides a threshold on the strength of physical noise below which reliable quantum computation can be guaranteed. However, directly applying the theorem to realistic noise has several challenges. One, the FT threshold is derived under oversimplified conditions that implicitly model a physical noise process as an incoherent error model with the same diamond distance. This leads to loose estimates of the logical performance when the noise has complex features such as coherence or strong correlations. Another is that diamond distance, which is usually invoked for assessing error rates in FT proofs, cannot be measured in a scalable way [9]. It has been shown that the resource overheads for a FT architecture depend critically on the precise relationship between the architecture and the underlying error model. While there are several well-studied error metrics, none of them can accurately predict the logical error rate of a quantum code, with predictions varying by several orders of magnitude [10]. In this work we ad-

dress this crucial deficiency prevalent in all of the known standard error metrics.

Here, we present a new figure of merit to predict the performance of concatenated codes, which can be measured efficiently using experimental protocols. As opposed to existing metrics such as average gate fidelity and diamond distance, our approach captures the interplay between the physical noise model and the choice of FT architecture. Our method leverages Randomized Compiling (RC) [11] to create an effective Pauli noise on the physical qubits, and then uses noise reconstruction (NR) techniques [12–14] to estimate Pauli error probabilities. Using these data, we then design a *logical estimator* that predicts the total probability of Pauli errors that a code cannot correct. While exactly computing this quantity is inefficient for a generic code, we introduce an efficient approximation to accurately estimate the total probability of uncorrectable errors for concatenated codes. We provide a bound on the efficiency and demonstrate the accuracy of our method through numerical simulations in several noise scenarios of interest. Finally, as an application, we demonstrate how the logical estimator pinpoints the selection of a suitable error correcting code for differing noise environments.

I. BACKGROUND

A wide class of Markovian noise processes are formally described by completely positive trace preserving (CPTP) maps [15]. There are several inequivalent ways to define the strength of noise modelled by a CPTP map \mathcal{E} . Of these, the two most widely used to study fault tolerance are the *average gate infidelity* [16–18]: $r(\mathcal{E}) = 1 - \int d\psi \operatorname{tr}(|\psi\rangle\langle\psi| \mathcal{E}(|\psi\rangle\langle\psi|))$, and the *diamond distance* [19–23]: $\|\mathcal{E} - \mathcal{I}\|_{\diamond} = \max_{\rho} \|(\mathcal{E} \otimes \mathcal{I})\rho - \rho\|_1$. While the average gate infidelity can be efficiently estimated using randomized benchmarking [24–27], the diamond distance satisfies mathematical properties that are needed in FT proofs [28–30]. Other standard error metrics include the 2-norm [31], Bures distance [32], Uhlmann fi-

delity [33], unitarity [34], channel entropy [35, 36] and the adversarial error probability [7]. None of these reflect the logical performance of a code [10, 37].

The net effect of a physical noise process \mathcal{E}_0 together with a quantum error correction (QEC) routine using an $[[n, k]]$ stabilizer code [38] is captured by the *effective logical channel* \mathcal{E}_1^s [39] acting on an encoded state $\bar{\rho}$ as:

$$\mathcal{E}_1^s(\bar{\rho}) = R_s \Pi_s \mathcal{E}_0(\bar{\rho}) \Pi_s R_s^\dagger / \Pr(s), \quad (1)$$

where $\Pr(s)$ is the probability of measuring the syndrome outcome s , Π_s is the syndrome projector and R_s is the corresponding recovery. The average logical channel $\bar{\mathcal{E}}_1$ is given by [10, 40]

$$\bar{\mathcal{E}}_1(\bar{\rho}) = \sum_s \Pr(s) \mathcal{E}_1^s(\bar{\rho}). \quad (2)$$

While physical error rates are measured by noise-metrics on \mathcal{E}_0 , logical error rates are measured on $\bar{\mathcal{E}}_1$.

Concatenated quantum codes are a popular family of codes of increasing sizes [41], and are often used to guarantee error suppression in fault tolerance proofs [7, 42]. Physical qubits of a code $\mathcal{C}_{\ell+1}$ are encoded using a code \mathcal{C}_ℓ , for $1 \leq \ell \leq L-1$, yielding a *level- L* concatenated code. The recursive encoding structure is represented by a tree where the i -th node at a depth $(L - \ell)$ denotes a quantum error correcting code block $\mathcal{C}_{\ell,i}$. The subtree of the node is itself a concatenated code, denoted by $\mathcal{C}_{\ell,i}^*$, consisting of $(n^\ell - 1)/(n - 1)$ code blocks. There are $n - 1$ independent stabilizer measurements corresponding to each of the code-blocks of $\mathcal{C}_{\ell,i}^*$. The resulting error syndrome $s(\mathcal{C}_{\ell,i}^*)$ has $(n^\ell - 1)$ bits, which can be grouped into subsets of $n - 1$ bits that are identified by the code-blocks. We identify the subset of syndrome bits obtained by measurements on a code-block $\mathcal{C}_{\ell,j}$ by $s(\mathcal{C}_{\ell,j})$.

We consider the following iterative routine for quantum error correction in concatenated codes. For each level $\ell = 1, \dots, L$: (i) syndromes are extracted for each code block $\mathcal{C}_{\ell,1}, \dots, \mathcal{C}_{\ell,n}$, and (ii) a minimum-weight correction [43] is applied in each case. Although we assume the popular choice of minimum-weight decoder in (ii), the methods prescribed in this work can be adapted to any lookup table decoder [44]. Hence, the correction applied at any level depends on the syndrome history of the code blocks in the lower levels.

The effective channel for a level- ℓ concatenated code can also be computed in a recursive fashion, i.e., using eq. (1) where \mathcal{E}_0 is replaced by effective channel on the level- $(\ell - 1)$ code blocks, i.e., $\mathcal{E}_{\ell-1,1}^s \otimes \dots \otimes \mathcal{E}_{\ell-1,n}^s$ [39, 45]. The performance of the level- ℓ concatenated code can be quantified [10] by the infidelity $r(\bar{\mathcal{E}}_\ell) = \sum_s \Pr(s) r(\mathcal{E}_\ell^s)$ of the average logical channel $\bar{\mathcal{E}}_\ell$. For concatenated codes, it is possible to calculate both $\Pr(s)$ and the effective channel \mathcal{E}_ℓ^s . However, as the number of syndromes grow exponentially with the number of levels, Monte Carlo sampling techniques described in section G of the appendix can be used to estimate this average.

II. METHODS

While the special setting of Pauli errors drastically simplifies the predictability problem, realistic noise processes are nonetheless poorly described by Pauli error models. To circumvent this problem, we recall a straightforward application of RC [11] to fault tolerant circuits, that allows us to model the effect of complex noise processes by simple Pauli errors. In other words, RC ensures that there is no effect on the logical error rate from parameters of the physical channel other than the Pauli error probabilities. The physical twirling gates required to do RC can be absorbed into the logical gadgets of the FT circuits, at no additional cost in overhead. We provide explicit details of the procedure in the appendix section B.

With a noise model described by Pauli errors, we first develop the background needed to define notion of a *logical estimator* that can accurately predict the logical error rate. A stabilizer code and a decoder pair is designed to correct a target set of errors \mathcal{E}_C , called *correctable errors* [46, 47]. Errors not in this set, i.e., uncorrectable errors, contribute to the logical error rate. Ideally, we want to estimate the total probability of all uncorrectable errors, which can be obtained by adding the probabilities of correctable errors and subtracting the result from one:

$$p_u(\mathcal{C}) = 1 - \sum_{E \in \mathcal{E}_C} \chi_{E,E}, \quad (3)$$

where $\chi_{P,Q}$ is the element corresponding to the Pauli operators P and Q , in the chi-matrix representation [48] of the physical noise process. For Pauli error models, p_u is identical to the logical infidelity, while for generic CPTP maps, a precise relationship is presented in section A of the appendix. While on the one hand, the average gate infidelity r accounts for the effect of only the trivial correctable error \mathbb{I} , p_u on the other hand captures all the degrees of freedom that are relevant to the logical error rate. However, an exact computation of p_u is intractable in general.

A correctable error E_ℓ for the concatenated code \mathcal{C}_ℓ^* falls into one of the two categories: either (i) it is corrected within the lower level code-blocks $\mathcal{C}_{\ell-1,1}, \dots, \mathcal{C}_{\ell-1,n}$, or (ii) it has a non-trivial correction applied by the decoder of the level- ℓ code-block $\mathcal{C}_{\ell,1}$. Adding up the contributions to $1 - p_u(\mathcal{C}_\ell^*)$ from cases (i) and (ii) respectively, we find

$$1 - p_u(\mathcal{C}_{\ell,1}^*) = \prod_{j=1}^n (1 - p_u(\mathcal{C}_{\ell-1,j}^*)) + \Gamma(\mathcal{C}_{\ell,1}^*), \quad (4)$$

where $\Gamma(\mathcal{C}_{\ell,1}^*) = \sum_{E \in \mathcal{E}_C \setminus \mathbb{I}} \Pr(\otimes_{j=1}^n E_{\ell-1,j})$. An exact computation of $\Gamma(\mathcal{C}_{\ell,1}^*)$ involves enumerating all possible syndrome outcomes for the level- ℓ concatenated code.

Our *logical estimator*, denoted by \tilde{p}_u , is the result of estimating p_u using an efficient approximation for $\Gamma(\mathcal{C}_{\ell,1}^*)$ for concatenated codes. In particular, we use a coarse

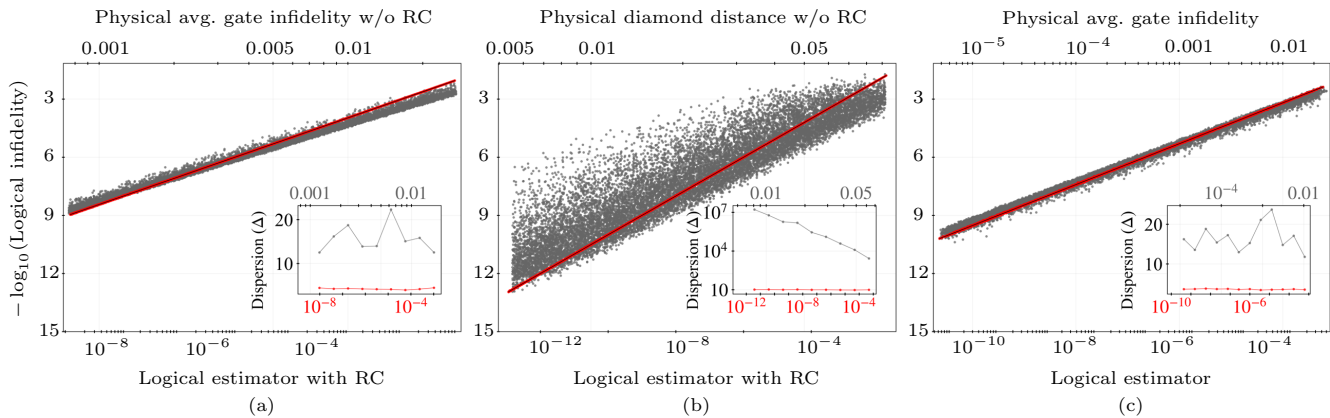


FIG. 1: Predictability of logical infidelity for level-2 concatenated Steane code. Figures 1(a,b) compare the predictive powers of our logical estimator (red) against two standard error metrics (gray): the average gate infidelity (a) and the diamond distance (b), under an ensemble of 18000 CPTP maps. Each point $p = (x_p, y_p)$ corresponds to a physical noise process; x_p is its physical error metric and y_p , its logical error rate. The dispersion of points, quantified as Δ in the insets, indicates the predictive power of the physical error metric. While logical error rates can vary over several orders of magnitude with respect to standard error metrics, our logical estimator is strongly correlated with the logical error rate. (c): Correlated Pauli error model.

grained estimate of the probability of a syndrome outcome – a joint probability distribution over $\mathcal{O}(n^\ell)$ syndrome bits – calculated as a product of marginal probability distributions over the n code blocks at level $(\ell - 1)$. This procedure is recursed through the ℓ levels of the concatenated code. A detailed derivation of the logical estimator is provided in section C of the appendix.

For i.i.d Pauli error models with sufficiently small single-qubit infidelity r_0 , the quality of approximation is: $|\bar{r}_\ell - \tilde{p}_u| \leq n_C^{\ell+1} r_0^{2+\lfloor (d_C+1)/2 \rfloor}$. Here, d_C and n_C describe the distance and the size of a codeblock of a level- ℓ concatenated code. For instance, using an i.i.d depolarizing error model with $r_0 = 10^{-3}$ and the level-2 concatenated Steane code, the above expression yields $|\bar{r}_2 - \tilde{p}_u| \leq 5 \times 10^{-10}$. This is validated by numerics: $\tilde{p}_u = 4.24 \times 10^{-9}$ and $\bar{r}_2 = 4.20 \times 10^{-9}$. Notably, the time complexity of computing \tilde{p}_u for the concatenated code: $\mathcal{O}(4^{n_C+\ell} n^\ell)$, scales polynomially in the total number of physical qubits, i.e., scaling as n^ℓ , whereas an exact computation of p_u would scale doubly exponentially in ℓ . An analysis of the quality and efficiency of the approximation, can be found in sections D and E, respectively, of the appendix.

III. RESULTS AND DISCUSSION

We provide numerical evidence to highlight the improvements offered by our methods developed for optimizing FT schemes. We begin with the task of accurately predicting the performance of concatenated Steane codes. We perform numerical simulations of quantum error correction in the RC and non-RC settings under a large ensemble of random CPTP maps applied to the physical qubits. Following Ref. [10], we generate a single qubit

CPTP map \mathcal{E} from its Stinespring dilation: a random unitary matrix U of size (8×8) , given by $U = e^{-iHt}$ for a complex Hermitian matrix H whose entries are sampled from a Gaussian distribution of unit variance, centred at 0. We vary the time parameter t between 0.001 and 0.1 to vary the noise strength.

Figure 1 shows that logical error rates can vary wildly across physical noise processes with fixed infidelity and diamond distance respectively, in agreement with the work in Ref. [10]. The variation, captured by the amount of dispersion in the scatter plots, is quantified using a simple measure – the ratio of the minimum and the maximum logical error rates across channels of similar physical error rate, denoted by Δ . In other words, we partition the range of physical error rates into bins b_i and use $\Delta(b_i)$ to quantify the amount of dispersion: $\Delta(b_i) = (1/|b_i|) (\max_{p \in b_i} y_p) / (\min_{p \in b_i} y_p)$, where $|b_i|$ is the number of channels in the bin b_i . The large fluctuations in the logical error rates can be attributed to two extreme features of the error-metrics. While infidelity controls only one parameter out of the many that specify a noise process, diamond distance, on the other hand, suffers from being sensitive to the details of a noise process that are irrelevant to the logical error rate. In addition, standard error metrics can only reveal intrinsic properties of the underlying noise process, that are agnostic to the choice of an error correcting code.

Logical estimator with RC, in contrast, is very highly correlated with the logical error rate. This improvement can be attributed to two features. First, RC provides a drastic reduction from $\mathcal{O}(12^n)$ parameters that specify an n -qubit Markovian noise process to $\mathcal{O}(4^n)$ Pauli error probabilities. Second, unlike standard error metrics, \tilde{p}_u carefully accounts for Pauli error probabilities that contribute to the logical error rate. Section F of the

appendix shows drastic gains in predictability using the logical estimator with RC, over standard error metrics, for the class of coherent errors.

The special setting of i.i.d noise hides the drastic advantages provided by \tilde{p}_u in predicting logical infidelity because the dominant contribution to \tilde{p}_u comes from $\chi_{0,0}$, which is also well captured by r . However, for correlated error-models, given only $\chi_{0,0}$, the uncertainty on the logical error rate ranges between the extremities, 0 and 1, achieved when all the multi-qubit errors are correctable, and uncorrectable, respectively. While r is completely insensitive to either of these scenarios, \tilde{p}_u in contrast helps distinguish between them, thereby providing a far more accurate estimate of the logical error rate.

We support the above argument by numerical studies of correlated Pauli error models generated from a convex combination of an i.i.d process of infidelity r_0 and multi-qubit interactions. While the i.i.d component \mathcal{E}_{iid} is specified by single qubit error probabilities, multi-qubit interactions are specified by an arbitrary subset \mathfrak{S} , so, $\mathcal{E}_{\text{cor}}(\rho) = \sum_{P \in \mathfrak{S}} \chi_{P,P} P \rho P$, where $\chi_{P,P}$ is sampled from the normal distribution with mean and variance $4^n r_0$. The combined Pauli error model is therefore given by $\mathcal{E}(\rho) = q\mathcal{E}_{\text{iid}}(\rho) + (1-q)\mathcal{E}_{\text{cor}}(\rho)$, where $0 \leq q \leq 1$. Explicitly setting $\chi_{0,0}$ followed by appropriate normalization, ensures that the infidelity of the above noise model is r_0 . Figure 1(c) highlights the importance of the logical estimator over the standard infidelity error metric for predicting the performance of the concatenated Steane code under correlated Pauli noise processes.

A. Logical estimator using limited NR data

Even in the absence of correlations across the n -qubit code blocks of a concatenated code, we require $\mathcal{O}(4^n)$ Pauli error rates from NR to compute \tilde{p}_u . Extracting this exponential sized NR dataset is a challenge for experimentalists. Refs. [14, 49] describe how to extract the leading K Pauli error probabilities in a noise process, where $K \ll 4^n$. We want to combine a handful of leading Pauli error rates extracted by NR with a simple method to extrapolate the remaining ones. We define the probability of a Pauli error Q that is not given in the NR dataset as

$$\Pr(Q) = (1 - r_0)^{n - \text{wt}(Q)} (r_0/3)^{\text{wt}(Q)}, \quad (5)$$

where $\text{wt}(Q)$ is the Hamming weight of Q , and r_0 is derived from the infidelity of the noise process: $r = 1 - (1 - r_0)^n$. We construct an adversarial example of an error model where the above extrapolation is unlikely to perform well by setting some multi-qubit error probabilities that violate eq. (5). Furthermore, when errors are sampled uniformly from the set of correctable and uncorrectable errors, we observe maximum fluctuations in the logical error rate. However, Fig. 2 presents strong numerical evidence indicating that the simple extrapolation works well in practice even for the adversarial example.

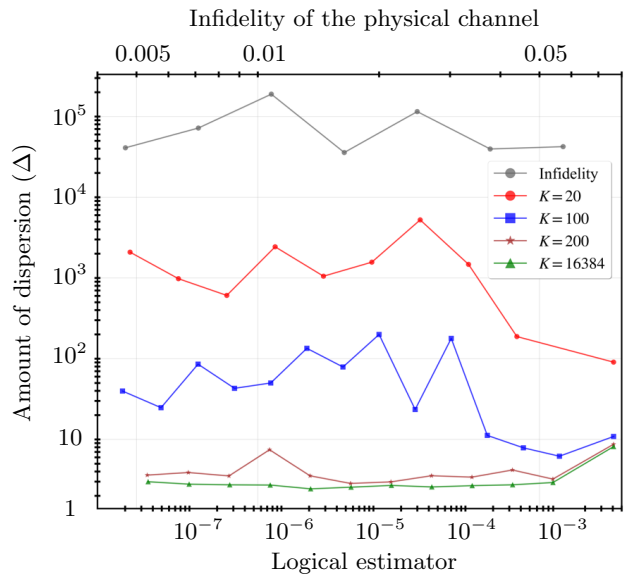


FIG. 2: Accuracy of the logical estimator based on limited NR data, using a level-2 concatenated Steane code for an ensemble of about 15000 random correlated Pauli channels. The accuracy, quantified by Δ , improves sharply with the number of Pauli error rates (K) extracted using NR. We observe that for $K = 200$, which is about 1.2% of all Pauli error rates on the Steane code block, the accuracy closely matches the logical estimator computed using all NR data, i.e., $K = 4^7$.

B. Code selection

Selecting a quantum error correcting code that has the smallest logical error rate under an existing physical noise process is a crucial step in optimizing resources for fault tolerance. To demonstrate the efficacy of the logical estimator for this problem, we consider an example of an error model and two different error-correcting codes: (i) concatenated Steane code and (ii) concatenated version of a $[[7, 1, 3]]$ code used in Ref. [2] that we refer to as a *Cyclic code*. The error model is obtained from a Pauli twirl on the i.i.d application of the CPTP map $\mathcal{E} : \rho \mapsto p_I \rho + \sum_{Q \in \{X, Y, Z\}} p_Q e^{-i\theta Q} \rho e^{i\theta Q}$, where $p_Y = p_X p_Z$, $p_I = 1 - p_X - p_Y - p_Z$ and set a bias specified by $\eta = p_Z/p_X$. Based on Ref. [2], we expect the Steane code to outperform the Cyclic code in one noise regime, and the converse in a different regime. Our tool is successful if it produces a lower value of \tilde{p}_u for the code with lower logical infidelity, for any noise rate. Lastly, to compute the logical estimator as well as the logical error rate estimates, we use a bias-adapted minimum-weight decoder that assigns weights η , η , and 1 to each Pauli error of type X , Y , and Z , respectively.

Our results presented in Fig. 3 show that the logical estimator correctly identifies the optimal code for all values of the physical error rate (bias). Furthermore, it also

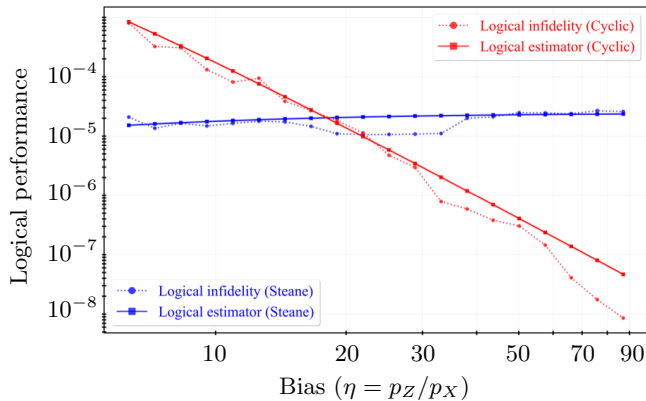


FIG. 3: Using the logical estimator to select an optimal code. The above figure demonstrates the use of our tool in selecting an optimal error correcting code under a biased Pauli error model. The choices of codes is between the level-3 concatenated versions of the Steane code and the cyclic code. While the solid lines depict the values of the logical estimator \tilde{p}_u , the dashed lines correspond to the logical error rates estimated using numerical simulations. We observe that \tilde{p}_u accurately selects the optimal code for all noise rates.

replicates the functional form of the logical error rate, showing that the performance gain from the Cyclic code over the Steane code increases with the bias.

IV. CONCLUSIONS

We have shown how experimental data from NR, even limited data, can be used to successfully predict the logical performance of FT architectures based on concatenated codes. It can be used to precisely and efficiently estimate the resource overhead required to achieve a target logical error rate [2, 50, 51] for implementing quantum algorithms. Along with informing the choice of an

optimal code for an underlying physical noise process, the logical estimator provides directives for other components in a FT scheme, such as a decoder. Different lookup table decoders can be compared using our logical estimator, similar to the work in Refs. [52–54].

Our scheme relies on RC to yield a Pauli error model, and although in theory this requires twirling with the full Pauli group, it has been observed in practice that a handful of random compilations of the original circuit are sufficient to achieve an almost Pauli-like effective noise process [55, 56]. A natural question that follows is whether RC also mitigates the impact of physical noise on the logical qubit. There is no persistent trend across the general class of Markovian noise processes, and in some cases, RC degrades the performance of the code. Developing noise tailoring techniques that guarantee an improvement to the performance as well as predictability is an interesting problem for future research.

Although the methods and techniques presented in the paper address generic noise processes, there are a number of roadblocks in broadening the scope of this study beyond concatenated codes, where the complexity of computing the logical estimator grows exponentially with the size of the code. In addition, further research is needed to extend these ideas to the context of multiple logical qubits.

ACKNOWLEDGMENTS

We thank Daniel Gottesman, Joel Wallman and Stefanie Beale for their valuable inputs. This research was undertaken thanks in part to funding from the Canada First Research Excellence Fund. Research was partially sponsored by the ARO and was accomplished under Grant Number: W911NF-21-1-0007. SDB acknowledges support from the Australian Research Council (ARC) via the Centre of Excellence in Engineered Quantum Systems (EQuS) project number CE170100009.

Appendix A: Logical fidelity and correctable errors

The average logical channel \mathcal{E}_1^s , defined in eq. 1, summarizes the effect of quantum error correction on a physical noise process \mathcal{E}_0 affecting an encoded state $\bar{\rho}$. In this section, we derive a closed form expression for the average logical channel in terms of the physical channel and the error correcting code parameters. Similar derivations have appeared in [39, 40, 57], however, we present ours for the sake of completeness.

The action of the average logical channel defined in eq. 2 on the logical state is

$$\begin{aligned}
\bar{\mathcal{E}}_1(\bar{\rho}) &= \sum_s \Pr(s) \mathcal{E}_1^s(\bar{\rho}), \\
&= \sum_s R_s \Pi_s \mathcal{E}_0(\bar{\rho}) \Pi_s R_s \\
&= \sum_s \sum_{i,j} \chi_{i,j} R_s \Pi_s P_i \bar{\rho} P_j \Pi_s R_s \\
&= \sum_s \sum_{\substack{i,j \\ s(P_i)=s(P_j):=s}} \chi_{i,j} R_s P_i \bar{\rho} P_j R_s,
\end{aligned} \tag{A1}$$

where in the last line we used the fact that $\Pi_s P_i = P_i \Pi_{s \oplus s(P_i)}$. In other words, whenever $s \neq s(P_i)$, the corresponding projector $\Pi_{s \oplus s(P_i)}$ annihilates the encoded state $\bar{\rho}$.

The chi matrix $\bar{\chi}$ of the effective logical channel defined by

$$\mathcal{E}_1(\bar{\rho}) = \sum_{l,m} \bar{\chi}_{lm} \bar{P}_l \bar{\rho} \bar{P}_m, \tag{A2}$$

where \bar{P}_l and \bar{P}_m are logical operators of the code; can be extracted from eq. A1.

The total probability of errors successfully corrected by the decoder: $\bar{\chi}_{00}$, can be estimated from the following observation. An error whose syndrome is s is corrected if the net effect of applying the error along with a recovery prescribed by the decoder results in an effective action of a stabilizer. In other words, all the terms in eq. A1 where $R_s P_i$ and $P_j R_s$ are stabilizers contribute to $\bar{\chi}_{00}$. So,

$$\bar{\chi}_{0,0} = \sum_{\substack{E, E' \in \mathcal{E}_C \\ s(E)=s(E'), \bar{E}=\bar{E}'}} \phi(E) \phi^*(E') \chi_{E, E'}, \tag{A3}$$

where \bar{E} is the logical component in the decomposition of E with respect to the Stabilizer group and $\phi(E)$ is specified by $R_{s(E)} E = \phi(E) S$ for any Pauli error E and some stabilizer S . The average logical infidelity \bar{r} is then given by $1 - \bar{\chi}_{00}$.

When a Pauli error is not correctable, the effect of applying a recovery yields a logical operator. Hence, in general

$$\bar{\chi}_{l,m} = \sum_{\substack{E, E' \in \mathcal{E}_C \\ s(E)=s(E'), \bar{E}=\bar{E}'}} \phi(E, l) \phi^*(E', m) \chi_{E \bar{P}_l, \bar{P}_m E'}. \tag{A4}$$

where $R_{s(E)} E \bar{P}_l = \phi(E, l) S$, for $l \in \{0, 1, 2, 3\}$, any Pauli error E and some stabilizer S .

Appendix B: Quantum error correction with randomized compiling

In this section, we discuss how randomized compiling (RC) can be performed in fault tolerant circuits. Note that a Pauli error P can be decomposed with reference to a stabilizer code: $P = \bar{P} S_P E_P$, where S_P is an element of the stabilizer group \mathcal{S} , \bar{P} is a logical Pauli operator in $\mathcal{L} = \mathcal{N}(\mathcal{S})/\mathcal{S}$, and E_P is an element of $\mathcal{N}(\mathcal{L})/\mathcal{S}$, usually called a pure error [45, 58]. Unlike pure errors, stabilizers and logical operators commute with QEC routines. A Pauli error P can be compiled into QEC resulting in a new quantum error correction routine $QEC(P)$ in which the input to the decoder corresponding to a syndrome outcome s is $s \oplus s(P)$ [59, 60].

In fault tolerant circuits, each logical gate \bar{G} is sandwiched between QEC routines. Following the prescription in [11], we divide logical gates into two sets: \mathcal{S}_1 and \mathcal{S}_2 , calling them easy and hard gates respectively. A crucial requirement for \mathcal{S}_1 and \mathcal{S}_2 is

$$\bar{G} T \bar{G}^\dagger QEC = QEC(T) \bar{C} \tag{B1}$$

for all easy logical gates $\bar{C} \in \mathcal{S}_1$, n -qubit Pauli gates T and hard gates \bar{G} . Recall that $QEC(T)$ refers to the compilation of the Pauli gate T in the QEC routine, discussed in sec. I. It follows from

$$\bar{G} T \bar{G}^\dagger QEC = \bar{G} \bar{T} \bar{G}^\dagger S_T E_T QEC \tag{B2}$$

$$= \bar{G} \bar{T} \bar{G}^\dagger QEC(E_T), \tag{B3}$$

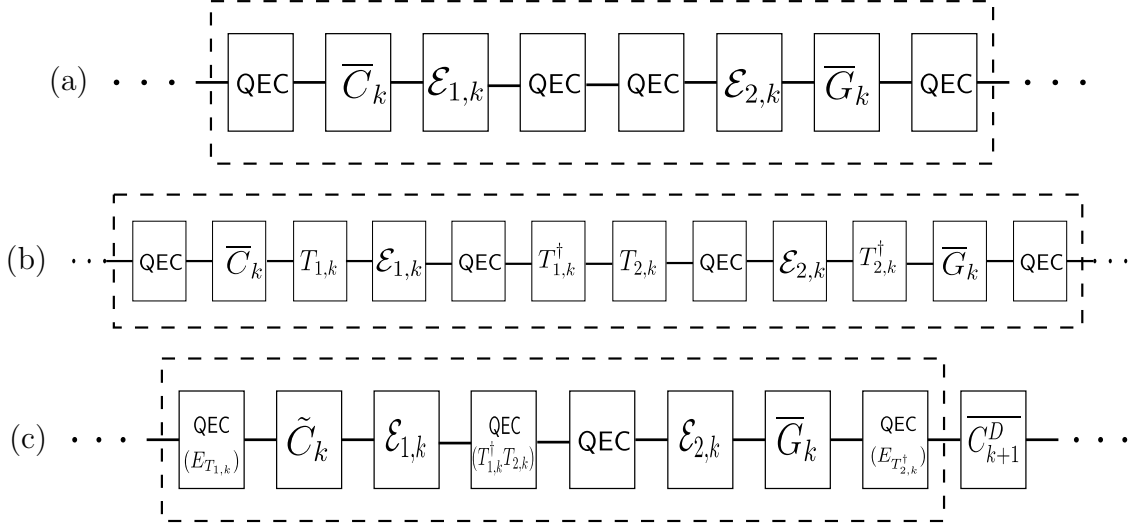


FIG. 4: Compiling twirling (random physical Pauli) gates into fault tolerant gadgets. Figure (a) shows the noisy gates in the k -th clock cycle of a fault tolerant quantum algorithm presented in the standard form prescribed in [11]. Twirling gates are inserted in figure (b) to tailor the noise processes to Pauli errors. These gates are compiled into existing gates by replacing easy gates by their dressed versions in figure (c).

where, in eq. B2 we have used the decomposition of Pauli gates with reference to a stabilizer code. Note that the expression $\overline{G} \overline{T} \overline{G}^\dagger$ in eq. B3 is guaranteed to be an easy gate for a choice of easy and hard gate sets in [11].

Fig. A.2(a) shows a canonical presentation of a quantum circuit, where the k -th clock cycle is composed of an easy gate \overline{C}_k and a hard gate \overline{G}_k , sandwiched between QEC routines. Noise processes affecting easy and hard gates are denoted by $\mathcal{E}_{1,k}$ and $\mathcal{E}_{2,k}$ respectively. These complex processes can be tailored to Pauli errors by inserting Pauli gates $T_{1,k}, T_{1,k}^\dagger, T_{2,k}, T_{2,k}^\dagger$. However, to guarantee that they be applied in a noiseless fashion, we compile them into the existing gates in the fault tolerant circuit. This is achieved in two steps. First, $T_{1,k}^\dagger$ and $T_{2,k}$ are compiled into QEC following $\mathcal{E}_{1,k}$, resulting in $QEC(T_{1,k}^\dagger T_{2,k})$. Second, $T_{2,k}^\dagger$ is propagated across \overline{G}_k , and compiled with $QEC \overline{C}_{k+1} T_{k+1}$, resulting in a *dressed gate* $\overline{C}_{k+1}^D = \overline{G}_k T_k \overline{G}_k^\dagger QEC \overline{C}_{k+1} T_{k+1}$. It follows from eq. B1 that \overline{C}_{k+1}^D is equivalent to quantum error correction followed by an easy gate.

Fig. A.2(c) shows the result of compiling all of the twirling gates into the easy gates and quantum error correction routines. Note that the compiled circuit is logically equivalent to the original circuit in the absence of noise. However, in the presence of noise, the average output of the circuit is dictated by the performance of $QEC(T)$ averaged over the different choices of Pauli gates T . This is what we refer to as QEC in the *RC setting*. In practice, this average performance can be achieved by repeating every iteration (shot) of the algorithm with a different Pauli operation compiled into the constituent QEC routines. For the purpose of numerical simulations in this paper, we have used the performance of the QEC routine under the twirled noise process, as a proxy to the performance of QEC in the RC setting.

Appendix C: Logical estimator for concatenated codes

In this section we discuss the derivation for the logical estimator \tilde{p}_u used to predict the logical error rate under physical Pauli noise processes. A stabilizer code and a decoder pair is designed to correct a target set of errors, called *correctable errors* [46, 47] \mathcal{E}_C . For an $[[n, k]]$ code, \mathcal{E}_C can be partitioned into 2^{n-k} disjoint subsets $\mathcal{E}_{C,1}, \dots, \mathcal{E}_{C,2^{n-k}}$, each of which can be identified with a unique syndrome measurement outcome. The construction of the set $\mathcal{E}_{C,s}$ closely depends on the choice of a decoder. Recall that the output of a decoder on input syndrome s is a Pauli recovery operator R_s , i.e., $R_s \in \mathcal{E}_{C,s}$. A key observation to construct elements in $\mathcal{E}_{C,s}$ besides R_s is that any error of the form $R_s S$ where S is an element of the stabilizer group is also correctable, so, $\mathcal{E}_{C,s} = \{R_s S : S \in \mathcal{S}\}$. Uncorrectable errors cause the quantum error correction scheme to fail. We adopt the notation p_c to denote the total probability of

correctable errors:

$$p_c = \sum_{E \in \mathcal{E}_C} \chi_{E,E}, \quad (\text{C1})$$

and p_u to denote the total probability of uncorrectable errors: $p_u = 1 - p_c$. It is easy to note that p_u is an upper bound to the standard infidelity metric which is measured by randomized benchmarking, i.e., $r = 1 - \chi_{0,0}$:

$$p_u = r - \sum_{\substack{E \in \mathcal{E}_C \\ E \neq \mathbb{I}}} \chi_{E,E}. \quad (\text{C2})$$

In particular, for Pauli noise processes the following equations show that p_u is exactly the average *logical* infidelity \bar{r} .

$$\bar{r} = 1 - \sum_{\substack{E, E' \in \mathcal{E}_C \\ s(E)=s(E'), \bar{E}=\bar{E}'}} \chi_{E,E'} \quad (\text{C3})$$

$$= r - \sum_{\substack{E, E' \in \mathcal{E}_C, E, E' \neq \mathbb{I} \\ s(E)=s(E'), \bar{E}=\bar{E}'}} \chi_{E,E'} \quad (\text{C4})$$

$$= p_u - \sum_{\substack{E, E' \in \mathcal{E}_C, E \neq E' \\ s(E)=s(E'), \bar{E}=\bar{E}'}} \chi_{E,E'}. \quad (\text{C5})$$

A detailed derivation of eq. C3 is presented in section A of this appendix. The expressions in eqs. C4 and C5 point out a conceptual difference between infidelity and the uncorrectable error probability. While on the one hand, r accounts for the effect of only the trivial correctable error \mathbb{I} , p_u on the other hand captures many more degrees of freedom – including all other correctable errors in \mathcal{E}_C . Hence, we expect r to be a worse predictor of the logical infidelity than p_u .

It is generally infeasible to enumerate all the $\mathcal{O}(4^{n-k})$ correctable errors for an $[[n, k]]$ stabilizer code, to compute p_u exactly. Our logical estimator is the result of an efficient heuristic to approximate p_u , particularly for concatenated code families. Furthermore, its accuracy is provably high for uncorrelated Pauli error models.

While for concatenated codes, the number of physical qubits itself grows exponentially in the size of a code block n , we can exploit its encoding structure to simplify the complexity of computing p_u . However, it turns out that despite this simplification we cannot exactly compute p_u efficiently, i.e., in time that scales polynomially in the number of physical qubits. This leads us to resort to a heuristic method for a reasonable approximation of p_u for concatenated codes, described in the rest of this section. Here we present a method to measure and compute an approximation, denoted by $\tilde{p}_u(\mathcal{C}_\ell^*)$, to the probability of uncorrectable errors for a concatenated code \mathcal{C}_ℓ^* : $p_u(\mathcal{C}_\ell^*)$. For ease of notation we also define the quantities $p_c(\mathcal{C}_\ell^*) = 1 - p_u(\mathcal{C}_\ell^*)$ and $\tilde{p}_c(\mathcal{C}_\ell^*) = 1 - \tilde{p}_u(\mathcal{C}_\ell^*)$.

An error E_ℓ for the level ℓ concatenated code \mathcal{C}_ℓ^* can be expressed as a tensor product of Pauli errors $E_{\ell-1,i}$ for the level $\ell - 1$ codes $\mathcal{C}_{\ell-1,i}^*$:

$$E_\ell = \bigotimes_{i=1}^n E_{\ell-1,i}. \quad (\text{C6})$$

Let us define E_ℓ to be a correctable pattern if the above tensor product corresponds to an encoded version of a correctable error for the code block \mathcal{C}_ℓ . For example, $E_2 = \bar{X} \otimes \bar{\mathbb{I}}^{\otimes 6}$ is a correctable pattern for the $\ell = 2$ concatenated Steane code since $X \otimes \mathbb{I}^{\otimes 6}$ is a correctable error for the Steane code block.

A correctable error E_ℓ for \mathcal{C}_ℓ^* falls into one of the two categories: either (i) it is corrected within the lower level code-blocks $\mathcal{C}_{\ell-1,1}^*, \dots, \mathcal{C}_{\ell-1,n}^*$, or (ii) it has a non-trivial correction applied by the decoder of the level- ℓ code-block $\mathcal{C}_{\ell,1}$. Let us denote the contribution to $p_c(\mathcal{C}_\ell^*)$ from case (i) by Λ , while that from case (ii) by Γ ; so that

$$p_c(\mathcal{C}_\ell^*) = \Lambda(\mathcal{C}_\ell^*) + \Gamma(\mathcal{C}_\ell^*). \quad (\text{C7})$$

Case (i) implies that each of the errors $E_{\ell-1,i}$ are correctable errors for the codes $\mathcal{C}_{\ell-1,i}^*$. Therefore, the total probability of correctable errors in case (i) admits a recursive definition:

$$\Lambda(\mathcal{C}_\ell^*) = p_c(\mathcal{C}_{\ell-1,1}^*) p_c(\mathcal{C}_{\ell-1,2}^*) \cdots p_c(\mathcal{C}_{\ell-1,n}^*). \quad (\text{C8})$$

Recall that case (ii) is the total probability of non-trivial correctable patterns for \mathcal{C}_ℓ^* , i.e.,

$$\Gamma(\mathcal{C}_\ell^*) = \sum_{E \in \mathcal{E}_C \setminus \mathbb{I}} \Pr(E_\ell) , \quad (\text{C9})$$

$$= \sum_{E \in \mathcal{E}_C \setminus \mathbb{I}} \Pr(E_{\ell-1,1} \otimes E_{\ell-1,2} \otimes \dots \otimes E_{\ell-1,n}) \quad (\text{C10})$$

where we have used the fact that each correctable error corresponds to a pattern according to eq. C6. A logical error $E_{\ell-1,i}$ occurs on the codeblock $\mathcal{C}_{\ell-1,i}$ whenever the decoder fails in correcting the physical errors in such a way that the residual effect of the physical noise process affecting the qubits of $\mathcal{C}_{\ell-1,i}^*$ and the recovery operation applied by the decoder results in $E_{\ell-1,i}$. Let us denote the probability of the decoder for $\mathcal{C}_{\ell-1,i}^*$ to leave a residual $E_{\ell-1,i}$, conditioned on the syndrome measurements by $\Pr_{\mathcal{D}}(E_{\ell-1,i} | s(\mathcal{C}_{\ell-1,i}^*))$. We can rewrite eq. C10 as

$$\Gamma(\mathcal{C}_\ell^*) = \sum_{E \in \mathcal{E}_C \setminus \mathbb{I}} \sum_{s(\mathcal{C}_\ell^*)} \Pr(s(\mathcal{C}_\ell) | s(\mathcal{C}_{\ell-1,1}^*) \dots s(\mathcal{C}_{\ell-1,n}^*)) \prod_{j=1}^n \Pr_{\mathcal{D}}(E_{\ell-1,j} | s(\mathcal{C}_{\ell-1,j}^*)) , \quad (\text{C11})$$

$$= \sum_{E \in \mathcal{E}_C \setminus \mathbb{I}} \sum_{s(\mathcal{C}_\ell^*)} \Pr(s(\mathcal{C}_\ell) | s(\mathcal{C}_{\ell-1,1}^*) \dots s(\mathcal{C}_{\ell-1,n}^*)) \prod_{j=1}^n \Pr_{\mathcal{D}}(E_{\ell-1,j} | s(\mathcal{C}_{\ell-1,j}^*)) \Pr(s(\mathcal{C}_{\ell-1,j}^*)) , \quad (\text{C12})$$

where $\Pr(s(\mathcal{C}_\ell) | s(\mathcal{C}_{\ell-1,1}^*) \dots s(\mathcal{C}_{\ell-1,n}^*))$, is the conditional probability of measuring the syndrome outcomes $s(\mathcal{C}_\ell)$ on the codeblock \mathcal{C}_ℓ when the outcomes on the lower level code blocks $\mathcal{C}_{\ell-1,1}^*, \dots, \mathcal{C}_{\ell-1,n}^*$ are $s(\mathcal{C}_{\ell-1,1}^*), \dots, s(\mathcal{C}_{\ell-1,n}^*)$, respectively. Equivalently,

$$\Pr(s(\mathcal{C}_\ell) | s(\mathcal{C}_{\ell-1,1}^*) \dots s(\mathcal{C}_{\ell-1,n}^*)) = \Pr(s(\mathcal{C}_\ell) | \mathcal{E}_{\ell-1,1}^{s(\mathcal{C}_{\ell-1,1}^*)} \dots \mathcal{E}_{\ell-1,n}^{s(\mathcal{C}_{\ell-1,n}^*)}) . \quad (\text{C13})$$

A major hurdle in computing Γ using eq. C12 is the sum over an exponentially large set of syndrome outcomes for the concatenated code. To circumvent this difficulty, we will apply an efficient heuristic to approximate the probability in eq. C13. In essence, we will replace the conditional channel $\mathcal{E}_{\ell-1,i}^{s(\mathcal{C}_{\ell-1,i}^*)}$ by the average logical channel $\hat{\mathcal{E}}_{\ell-1,i}$, which is defined as

$$\hat{\mathcal{E}}_{\ell-1,i} = \sum_{s(\mathcal{C}_{\ell-1,i})} \Pr(s(\mathcal{C}_{\ell-1,i})) \mathcal{E}_{\ell-1,i}^{s(\mathcal{C}_{\ell-1,i})} \left[\hat{\mathcal{E}}_{\ell-2,1} \otimes \dots \otimes \hat{\mathcal{E}}_{\ell-2,n} \right] . \quad (\text{C14})$$

Note that $\hat{\mathcal{E}}_{0,j}$ is the physical noise model while $\hat{\mathcal{E}}_{1,j}$ is the exact average logical channel $\bar{\mathcal{E}}_{1,j}$. However, in general for $\ell \geq 2$, $\hat{\mathcal{E}}_\ell$ is a coarse-grained approximation for the exact average logical channel $\bar{\mathcal{E}}_\ell$. In other words, $\hat{\mathcal{E}}_{\ell-1,i}$ is computed using the knowledge of the syndrome bits measured only at level $\ell - 1$, while assuming the noise model: $\hat{\mathcal{E}}_{\ell-2,1} \otimes \dots \otimes \hat{\mathcal{E}}_{\ell-2,n}$, that accounts for the average effect of all syndrome measurements at lower levels.

Replacing the conditional channel $\mathcal{E}_{\ell-1,i}^{s(\mathcal{C}_{\ell-1,i}^*)}$ in eq. C12 by the average channel $\hat{\mathcal{E}}_{\ell-1,i}$ defined in eq. C14 allows us to approximate Γ by $\tilde{\Gamma}$ defined as follows:

$$\tilde{\Gamma}(\mathcal{C}_\ell^*) = \sum_{E \in \mathcal{E}_C \setminus \mathbb{I}} \sum_{s(\mathcal{C}_\ell)} \sum_{s(\mathcal{C}_{\ell-1,1}^*)} \dots \sum_{s(\mathcal{C}_{\ell-1,n}^*)} \Pr(s(\mathcal{C}_\ell) | \hat{\mathcal{E}}_{\ell-1,1} \dots \hat{\mathcal{E}}_{\ell-1,n}) \prod_{j=1}^n \Pr_{\mathcal{D}}(E_{\ell-1,j} | \hat{\mathcal{E}}_{\ell-1,j}) \Pr(s(\mathcal{C}_{\ell-1,j}^*)) , \quad (\text{C15})$$

$$= \sum_{E \in \mathcal{E}_C \setminus \mathbb{I}} \prod_{j=1}^n \Pr_{\mathcal{D}}(E_{\ell-1,j} | \hat{\mathcal{E}}_{\ell-1,j}) . \quad (\text{C16})$$

Denote $\mathcal{R}(s(\mathcal{C}_{\ell-1,i}), P)$ to be the set of n -qubit errors on which a lookup table decoder for the code block $\mathcal{C}_{\ell-1,i}$ leaves a residual logical error P when the error syndrome $s(\mathcal{C}_{\ell-1,i})$ is encountered. Now $\Pr_{\mathcal{D}}(E_{\ell-1,i} | \hat{\mathcal{E}}_{\ell-1,j})$ can be computed recursively:

$$\Pr_{\mathcal{D}}(E_{\ell-1,i} | \hat{\mathcal{E}}_{\ell-1,i}) = \sum_{Q \in \mathcal{R}(s(\mathcal{C}_{\ell-1,i}), E_{\ell-1,i})} \prod_{j=1}^n \Pr_{\mathcal{D}}(Q_{\ell-2,j} | \hat{\mathcal{E}}_{\ell-2,j}) . \quad (\text{C17})$$

Note that the probability of leaving a residual error at level 0 is simply specified by the physical noise model, i.e., $\Pr_{\mathcal{D}}(P | \hat{\mathcal{E}}_{0,j})$ is the probability of the Pauli error P on the physical qubit j . This concludes the method to efficiently compute $\tilde{\Gamma}$, an approximation to Γ .

Recall that the total probability of correctable errors is given by eq. C7. An approximation to $p_c(\mathcal{C}_\ell^*)$, is given by

$$\tilde{p}_c(\mathcal{C}_\ell^*) = \tilde{\Lambda}(\mathcal{C}_\ell^*) + \tilde{\Gamma}(\mathcal{C}_\ell^*) , \quad (\text{C18})$$

where $\tilde{\Gamma}$ defined in eq. C16 while $\tilde{\Lambda}$ is defined in a similar fashion to eq. C8:

$$\tilde{\Lambda}(\mathcal{C}_\ell^*) = \tilde{p}_c(\mathcal{C}_{\ell-1,1}^*)\tilde{p}_c(\mathcal{C}_{\ell-1,2}^*)\dots\tilde{p}_c(\mathcal{C}_{\ell-1,n}^*) . \quad (\text{C19})$$

Using the approximation in eq. C18, we can efficiently estimate the logical estimator \tilde{p}_u for concatenated codes.

Appendix D: Approximation quality for the uncorrectable error probability

In this section, we will quantify the accuracy of the approximating the uncorrectable error probability using \tilde{p}_u for concatenated codes. For simplicity, we will assume that the code-blocks in the concatenated code are all identical, and equal to a $[[n, 1, d]]$ quantum error correcting code, with $d \geq 3$. Recall that the distance of a level ℓ concatenated code scales as d^ℓ . We will use $t_\ell = \lfloor (d^\ell + 1)/2 \rfloor$ to denote the Hamming weight of the smallest uncorrectable error. Recall that \tilde{p}_u is defined recursively as the sum of two quantities: \tilde{Q}_1 and \tilde{Q}_2 . We will use δ_ℓ to denote the inaccuracy in computing p_u for a level ℓ concatenated code:

$$\delta_\ell = |p_u(\mathcal{C}_{\ell,1}^*) - \tilde{p}_u(\mathcal{C}_{\ell,1}^*)| , \quad (\text{D1})$$

and γ_ℓ to denote the inaccuracy in computing Γ :

$$\gamma_\ell = |\tilde{\Gamma}(\mathcal{C}_\ell^*) - \Gamma(\mathcal{C}_\ell^*)| . \quad (\text{D2})$$

Then it follows that

$$\delta_\ell \leq n\delta_{\ell-1} + \gamma_\ell . \quad (\text{D3})$$

The most important ingredient in computing δ_ℓ is γ_ℓ , defined in eq. D2. For simplicity we will compute γ_ℓ for the i.i.d depolarizing error model. However, for generic i.i.d Pauli error models, we can replace the depolarizing rate p in our analysis by the physical infidelity of the single qubit error model, r_0 . The extension to correlated Pauli error models remains unclear.

An i.i.d application of the depolarizing channel on n -qubits can be described by

$$\mathcal{E}(\rho) = \sum_{P \in \mathcal{P}_n} \chi_{P,P} P \rho P ,$$

such that $\chi_{P,P} = (1-p)^{n-|P|} \left(\frac{p}{3}\right)^{|P|} ,$ (D4)

where \mathcal{P}_n is the n -qubit Pauli group, $0 \leq p \leq 1$ is the depolarizing rate and $|P|$ is the Hamming weight of the Pauli error P . In this case, we will show that

$$\gamma_\ell = \mathcal{O}(n^{\ell-1} p^{t_{\ell-1}+2}) , \quad (\text{D5})$$

for a level ℓ concatenated code.

Combining eq. D5 with eq. D3, we arrive at an expression for δ_ℓ :

$$\delta_\ell = \mathcal{O}(n^{\ell-1} p^{2+\lfloor (d+1)/2 \rfloor}) , \quad (\text{D6})$$

where d is the distance of a code block.

In the rest of this section, we will derive eq. D5. Recall that eq. C16 outlines the approximation made by the heuristic to compute $\Gamma(\mathcal{C}_\ell^*)$. It involves replacing the knowledge of conditional channels $\mathcal{E}_{\ell-1,j}^s$ by the average channel, $\hat{\mathcal{E}}_{\ell-1,j}$. We will prove the scaling in eq. D5 two steps. First, is an observation that

$$\prod_{j=1}^n \Pr_{\mathcal{D}}(E_{\ell-1,j} | \hat{\mathcal{E}}_{\ell-1,j}) = \mathcal{O}(p^{t_{\ell-1}}) . \quad (\text{D7})$$

This follows from the fact that at least one of the errors $E_{\ell-1,j}$ in the error pattern $E_{\ell-1,1} \otimes \dots \otimes E_{\ell-1,n}$ must be non-identity. Note that a non-identity logical error is left as a residual when the decoder for the subsequent lower level fails. Such an event will not occur for errors whose weight is below $t_{\ell-1}$.

Second, by showing that

$$\begin{aligned} \Pr(s(\mathcal{C}_{\ell,i}) | \mathcal{E}_{\ell-1,1}^{s(\mathcal{C}_{\ell-1,1}^*)} \dots \mathcal{E}_{\ell-1,n}^{s(\mathcal{C}_{\ell-1,n}^*)}) \prod_{i=1}^n \Pr(s(\mathcal{C}_{\ell-1,j}^*)) = \\ \Pr(s(\mathcal{C}_{\ell,i}) | \hat{\mathcal{E}}_{\ell-1,1} \dots \hat{\mathcal{E}}_{\ell-1,n}) \prod_{i=1}^n \Pr(s(\mathcal{C}_{\ell-1,j}^*)) + \mathcal{O}(n^{\ell-1}p^2). \end{aligned} \quad (\text{D8})$$

Recall from eq. C14 that the average channel $\hat{\mathcal{E}}_{\ell,i}$ is defined recursively in terms of $\hat{\mathcal{E}}_{\ell-1,j}$. While the term corresponding to $s(\mathcal{C}_{\ell,i}) = 0$ describes the effect of stabilizers on the input state, the other terms include the effect of non-trivial errors. Note that a non-trivial error E_{ℓ} has weight at least $t_{\ell-1}$, equal to the weight of the smallest uncorrectable error of the concatenated code $\mathcal{C}_{\ell-1,j}^*$. Carrying this idea from level $\ell - 1$ to level 1, we find:

$$\hat{\mathcal{E}}_{\ell,i} = \mathcal{E}_{\ell,i}^{s(\mathcal{C}_{\ell,i})=0} \left[\hat{\mathcal{E}}_{\ell-1,1} \otimes \dots \otimes \hat{\mathcal{E}}_{\ell-1,n} \right] + \mathcal{O}(p^{t_{\ell-1}}), \quad (\text{D9})$$

$$= \left(\hat{\mathcal{E}}_{\ell-1,1} \otimes \dots \otimes \hat{\mathcal{E}}_{\ell-1,n} \right) + \mathcal{O}(p^{t_{\ell-2}}), \quad (\text{D10})$$

$$= \left(\hat{\mathcal{E}}_{1,1} \otimes \dots \otimes \hat{\mathcal{E}}_{1,n^{\ell-1}} \right) + \mathcal{O}(p^{t_1}), \quad (\text{D11})$$

where in eq. D10 we have used the fact that the leading contribution to the conditional channel for the trivial syndrome, is the physical channel itself. Equation D11 describes the recursion until level $\ell = 1$ where $\hat{\mathcal{E}}_{1,j} = \bar{\mathcal{E}}_{1,j}$.

Recall that the conditional channel for an error-syndrome $s(\mathcal{C}_{\ell-1,i}^*)$,

$$\mathcal{E}_{\ell-1,i}^{s(\mathcal{C}_{\ell-1,i}^*)} = \mathcal{E}_{\ell-1,i}^{s(\mathcal{C}_{\ell-1,i})s(\mathcal{C}_{\ell-2,1}) \dots s(\mathcal{C}_{\ell-2,n}) \dots s(\mathcal{C}_{1,1}) \dots s(\mathcal{C}_{1,n^{\ell-1}})}, \quad (\text{D12})$$

is defined by applying quantum error correction routines corresponding to the syndrome outcomes in the respective code-blocks of $\mathcal{C}_{\ell-1,i}^*$. Note that an error is detected (by means of a non-trivial syndrome outcome) in a code block at level ℓ when the decoder operating on the code block at level $\ell - 1$ leaves a non-trivial residue. Hence, for a leading order analysis, we will consider conditional channels that correspond to trivial syndromes in all the code-blocks except for those at level one, i.e., $s(\mathcal{C}_{\ell,i}) = 0$ for all $\ell > 1$ in eq. D12. In other words, we will consider errors that are corrected within the code blocks in level one:

$$\mathcal{E}_{\ell-1,i}^{s(\mathcal{C}_{\ell-1,i})=0, s(\mathcal{C}_{\ell-2,1})=0, \dots, s(\mathcal{C}_{\ell-2,n})=0, \dots, s(\mathcal{C}_{1,1}) \dots s(\mathcal{C}_{1,n^{\ell-1}})} = \mathcal{E}_{1,1}^{s(\mathcal{C}_{1,1})} \otimes \dots \otimes \mathcal{E}_{1,n^{\ell-1}}^{s(\mathcal{C}_{1,n^{\ell-1}})} + \mathcal{O}(p^{t_1}). \quad (\text{D13})$$

Using eqs. D11 and D13, we note that the quality of the approximation in eq. D8 can be bounded as follows:

$$\begin{aligned} & \left(\Pr(s(\mathcal{C}_{\ell}) | \mathcal{E}_1^{s(\mathcal{C}_{1,1})} \dots \mathcal{E}_1^{s(\mathcal{C}_{1,n^{\ell-1}})}) - \Pr(s(\mathcal{C}_{\ell}) | \hat{\mathcal{E}}_{1,1} \dots \hat{\mathcal{E}}_{1,n^{\ell-1}}) \right) \prod_{j=1}^{n^{\ell-1}} \Pr(s(\mathcal{C}_{1,j})) \\ &= \text{tr} \left[\Pi_{s(\mathcal{C}_{\ell})} \cdot \left((\mathcal{E}_1^{s(\mathcal{C}_{1,1})} \otimes \dots \otimes \mathcal{E}_1^{s(\mathcal{C}_{1,n^{\ell-1}})}) (\rho) - (\hat{\mathcal{E}}_{1,1} \otimes \dots \otimes \hat{\mathcal{E}}_{1,n^{\ell-1}}) (\rho) \right) \right] \prod_{j=1}^{n^{\ell-1}} \Pr(s(\mathcal{C}_{1,j})), \end{aligned} \quad (\text{D14})$$

$$= \sum_i \left[\left(\chi_{1,1}^{s(\mathcal{C}_{1,1})} \otimes \dots \otimes \chi_{1,n^{\ell-1}}^{s(\mathcal{C}_{1,n^{\ell-1}})} \right)_{i,i} - \left(\hat{\chi}_{1,1} \otimes \dots \otimes \hat{\chi}_{1,n^{\ell-1}} \right)_{i,i} \right] \text{tr} \left[\Pi_{s(\mathcal{C}_{\ell})} \cdot P_i \rho P_i \right] \prod_{j=1}^{n^{\ell-1}} \Pr(s(\mathcal{C}_{1,j})), \quad (\text{D15})$$

$$\leq n^{\ell-1} \max_{s \in \mathbb{Z}_2^{n-k}} \|\chi_1^s - \hat{\chi}_1\|_{\infty} \Pr(s), \quad (\text{D16})$$

where χ_1^s refers to the chi matrix of the conditional channel \mathcal{E}_1^s while $\hat{\chi}_1$ refers to the chi matrix of the average channel $\hat{\mathcal{E}}_1$. In eq. D16, we have used the matrix norm $\|A\|_{\infty}$ to refer to the maximum absolute value in the matrix.

To establish the scaling in eq. D8 it remains to show that

$$\max_{s \in \mathbb{Z}_2^{n-k}} \|\chi_1^s - \hat{\chi}_1\|_{\infty} \Pr(s) = \mathcal{O}(p^2). \quad (\text{D17})$$

Recall that the effective channel for a given syndrome s : \mathcal{E}_1^s , describes the composite effect of the physical noise process and quantum error correction conditioned on the measurement outcome s . Comparing eq. A1 to the general form in eq. A2, we find an expression similar to eq. A4:

$$[\chi_1^s]_{i,i} = \frac{1}{\Pr(s)} \sum_{\substack{E \in \mathcal{E}_C \\ s(E)=s}} \chi_{\bar{P}_i E, \bar{P}_i E}. \quad (\text{D18})$$

For the specific case of the depolarizing channel in D4 we can express $[\chi_1^s]_{i,i}$, $\Pr(s)$ and $\hat{\chi}_{i,i}$ as polynomials in the depolarizing rate p :

$$[\chi_1^s]_{i,i} = \frac{1}{\Pr(s)} \sum_{w=1}^n A_{i,w}^s (1-p)^{n-w} \left(\frac{p}{3}\right)^w, \quad (\text{D19})$$

$$\Pr(s) = \sum_i \sum_{w=1}^n A_{i,w}^s (1-p)^{n-w} \left(\frac{p}{3}\right)^w, \quad (\text{D20})$$

$$\hat{\chi}_{i,i} = \sum_s \sum_{w=0}^n A_{i,w}^s (1-p)^{n-w} \left(\frac{p}{3}\right)^w, \quad (\text{D21})$$

where $A_{i,w}^s$ is the number of Pauli errors Q of Hamming weight w on which the action of the decoder leaves a residual logical error \bar{P}_i . In other words, $Q = \bar{P}_i R_s S$ where R_s is the recovery operation prescribed by the decoder for the error-syndrome s and S is any stabilizer. We can use two simple facts about errors to simplify the coefficients $A_{i,w}^s$. First, since the only error of Hamming weight zero is the identity which has $s = 0$, we find $A_{i,0}^s = \delta_{s,0} \delta_{i,0}$. Second, since all errors of Hamming weight up to $\lfloor (d-1)/2 \rfloor$ are correctable, we find $A_{i,w}^s = \delta_{i,0} A_{0,w}^s$ for all $w \leq \lfloor (d-1)/2 \rfloor$. Using these simplifications,

$$[\chi_1^s]_{i,i} = \frac{1}{\Pr(s)} \left[(1-p)^{n-1} \left(\frac{p}{3}\right) A_{0,1}^s + \mathcal{O}(n^2 p^2) \right], \quad (\text{D22})$$

$$\Pr(s) = A_{0,1}^s (1-p)^{n-1} \left(\frac{p}{3}\right) + \mathcal{O}(n^2 p^2), \quad (\text{D23})$$

$$\hat{\chi}_{i,i} = \delta_{i,0} (1-p)^n + 3n(1-p)^{n-1} \left(\frac{p}{3}\right) \delta_{i,0} + \mathcal{O}(n^2 p^2). \quad (\text{D24})$$

It is now straightforward to see that eq. D17 follows from the above set of equations.

In summary, this section establishes that the approximation used by the heuristic to compute $\tilde{p}_u(\mathcal{C}_{\ell,1}^*)$, is accurate to $\mathcal{O}(n^{\ell+1} p^{2+\lfloor (d+1)/2 \rfloor})$ for the i.i.d depolarizing physical error model with error rate p . To get a sense for this approximation quality, we can plug in relevant numbers for an i.i.d Pauli error model and level-2 concatenated Steane code: $p = 10^{-3}$, $n = 7$, $\ell = 2$, $d = 3$. Numerical simulations of quantum error correction yield an estimate of the logical infidelity given by 4.2×10^{-9} . The analytical bound suggests that the logical estimator derived from the our heuristic method agrees with the logical infidelity up to $\mathcal{O}(10^{-11})$. However, the scaling suggests that the heuristic may not be accurate for large codes in the high noise regime. Nonetheless we have strong numerical evidence to support that the logical estimator predicts the functional form of logical infidelity.

Appendix E: Time complexity of computing \tilde{p}_u for concatenated codes

Recall that $\tilde{p}_u = 1 - \tilde{p}_c(\mathcal{C}_\ell^*)$, where $\tilde{p}_c(\mathcal{C}_\ell^*)$ is an approximation to the total probability of correctable errors. We will analyze the time complexity of the technique described in section C to compute $\tilde{p}_c(\mathcal{C}_\ell^*)$ here.

Note that $\tilde{p}_c(\mathcal{C}_\ell^*) = \tilde{\Lambda} + \tilde{\Gamma}$ where both $\tilde{\Lambda}$ and $\tilde{\Gamma}$ are defined recursively. So, if computing $\tilde{p}_c(\mathcal{C}_\ell^*)$ takes time τ_ℓ and computing $\tilde{\Gamma}$ takes time κ_ℓ , we have

$$\tau_\ell = n \tau_{\ell-1} + \kappa_\ell. \quad (\text{E1})$$

The recurrence relation in eq. C16 for computing $\tilde{\Gamma}(\mathcal{C}_\ell^*)$ implies

$$\kappa_\ell = 4n \kappa_{\ell-1} + \mathcal{O}(4^n), \quad (\text{E2})$$

$$= \mathcal{O}(4^{n+\ell} n^\ell). \quad (\text{E3})$$

Using the above solution in eq. E1, we find that

$$\tau_\ell = \mathcal{O}(4^{n+\ell} n^\ell). \quad (\text{E4})$$

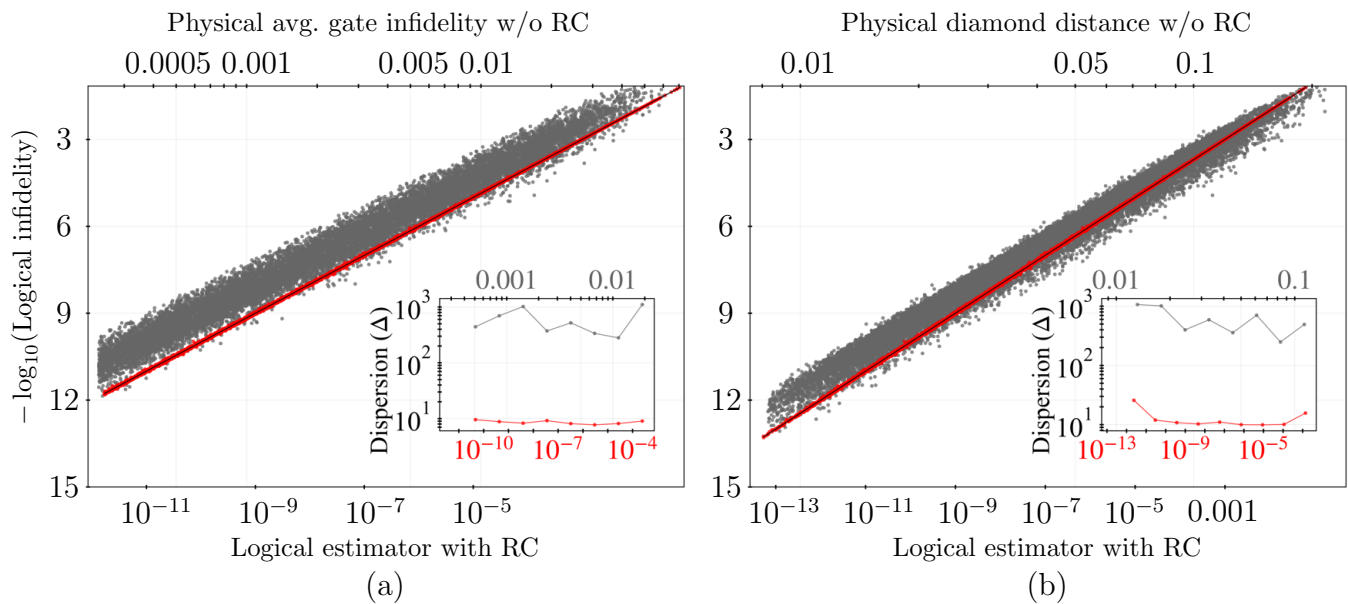


FIG. 5: Predicting the performance of level-2 concatenated Steane code under unitary errors. Figures (a) and (b) compare the predictive powers of our tool (red) with the standard error metrics: infidelity and the diamond distance, respectively, under an ensemble of 16000 random unitary channels. These are similar to figures 1(a) and 1(b) in the main text. The dispersion in the scatter corresponding to a metric (Δ in the insets) is indicative of its predictive power. The gains in predictability offered by our tool is drastic for the above case of unitary errors when compared to CPTP maps.

Appendix F: Predictability results for coherent errors

Numerical results presented in section III highlight the predictive power of the tools developed in this work with respect to the standard error-metrics, under random CPTP maps. Although CPTP maps encompass a wide range of physical noise processes, our method of generating random CPTP maps does not draw attention to an important class of noise processes – coherent errors – a special case of CPTP maps under which the evolution of a qubit is described by a unitary matrix. They occur due to imperfect control quantum devices and calibration errors [61, 62]. Various methods such as dynamical decoupling [63, 64], designing pulses using optimal control theory [65] and machine learning approaches [66] are used to mitigate these errors. However, each of these methods have their shortcomings and unitary errors continue to form a major part of the total error budget [67–69]. The methods presented in this paper will be particularly advantageous in these cases.

In this section we highlight the predictive power of our tool, over standard error metrics, under different coherent noise processes. We choose a simple class of coherent errors modeled by an unknown unitary U_i on each physical qubit i , of the form $U = e^{-i\frac{\delta}{2}\hat{n}\cdot\vec{\sigma}}$, where δ is the angle of rotation about an axis \hat{n} on the Bloch sphere. With a slight loss of generality, we will consider n -qubit unitary errors of the form $\otimes_{i=1}^n U_i$. We control the noise strength by rotation angles δ_i drawn from a normal distribution of mean and variance equal to μ_δ where $10^{-3} \leq \mu_\delta \leq 10^{-1}$.

Figure 5 shows that logical error rates vary over several orders of magnitudes across coherent errors with noise strength as measured by standard error-metrics such as infidelity and the diamond distance. In contrast, our tools provide an accurate prediction using the logical estimator developed in section C. Moreover, we observe a drastic gain in in predictability using our tools for this case of unitary errors, when compared to CPTP maps in figure 1 of the main text.

Appendix G: Importance sampling

A straightforward technique to estimate the logical error rate involves sampling syndrome outcomes according to the syndrome probability distribution for a quantum error correcting code and a physical noise process pair. However, there are serious drawbacks to this sampling method, due to the presence of rare syndromes – whose probability is typically less than the inverse number of syndrome samples. A detailed account of this can be found in [10] and in

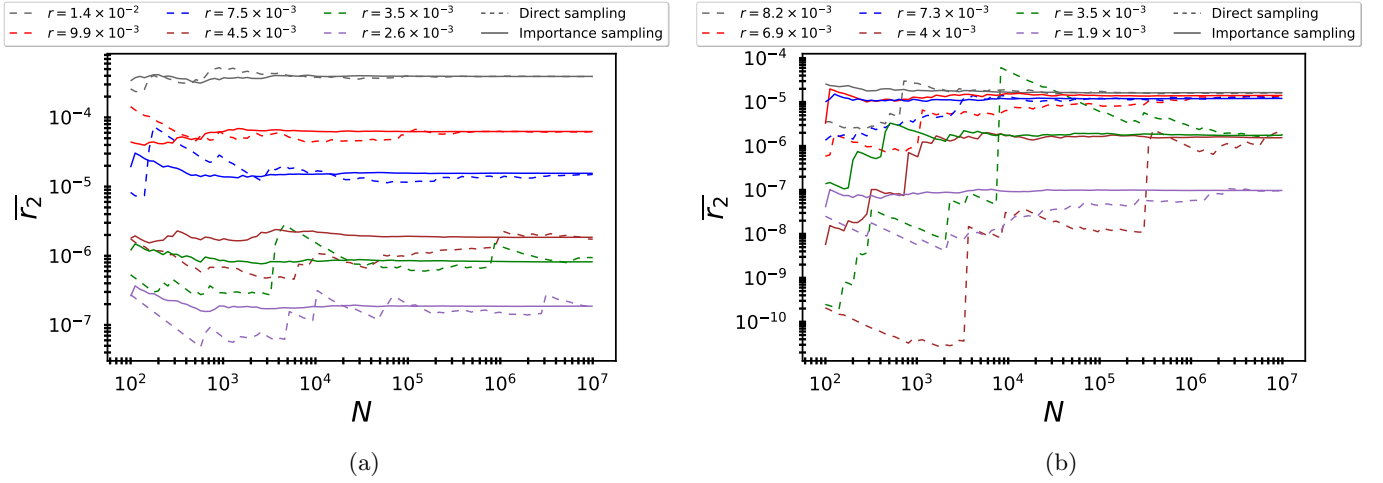


FIG. 6: The above figures highlight the rapid convergence rate of the importance sampler as compared to the direct sampler, under CPTP noise processes in Fig. 6(a) and coherent errors in Fig. 6(b). Each trend line in the figures is associated to a physical noise rate. While different colors are used to identify different physical error rates, the solid and dashed lines are used to distinguish between the sampling techniques. Note that while the direct sampler takes a large number of syndrome samples to provide a reliable estimate of $r(\mathcal{E}_\ell)$, the importance sampler achieves this task with far lesser syndrome samples. The speedup offered by importance sampling is quite drastic. The case for $r = 4 \times 10^{-3}$ in Fig. 6(b) is a good example. The direct sampler shows signs of convergence around 10^7 syndrome samples, whereas the importance sampler converges with just 10^4 samples. Notice however that with only 10^4 samples, the direct sampler underestimates $r(\mathcal{E}_\ell)$ by almost two orders of magnitude.

section 3.3 of [37]. We briefly review the technique here for completeness.

In summary the average logical error rate is grossly underestimated unless an unreasonably large number of outcomes are sampled. We will resort to an importance sampling technique proposed in [10], to improve our estimate of the average logical error rate. Previously, similar techniques have also been discussed for Pauli noise processes in [71, 72]. Instead of choosing to sample the syndrome probability distribution, we sample an alternate distribution $Q(s)$, which we will simply refer to as the *importance distribution*. The corresponding sampling methods with $\Pr(s)$ and $Q(s)$ will be referred to as *direct sampling* and *importance sampling* respectively.

The expression for the average logical error rate estimated by the importance sampler takes a form:

$$r(\hat{\mathcal{E}}_\ell) = \sum_{\hat{s}} r(\mathcal{E}_\ell^{\hat{s}}) \frac{\Pr(s)}{Q(s)}, \quad (\text{G1})$$

where \hat{s} is a random syndrome outcome drawn from the importance distribution $Q(s)$. The average estimated by importance sampling coincides with $r(\mathcal{E}_\ell)$ which is estimated by the direct sampling technique. The crucial difference between the two sampling techniques is that the variance of the estimated average can be significantly lowered by an appropriate choice for the importance distribution $Q(s)$, which in our case, takes the form

$$Q(s) = \frac{P(s)^{1/k}}{Z}, \quad (\text{G2})$$

where Z is a normalization factor

$$Z = \sum_s P(s)^{1/k}, \quad (\text{G3})$$

and $k \in (0, 1]$ is chosen such that the total probability of non-trivial syndrome outcomes, $s \neq 00 \dots 0$, is above a fixed threshold λ_0 , i.e.,

$$\sum_{s \neq 00 \dots 0} \frac{\Pr(s)^{1/k}}{Z} \geq \lambda_0. \quad (\text{G4})$$

Figure 6 shows that our heuristic for the importance distribution provides a rapid convergence to $r(\bar{\mathcal{E}}_\ell)$, when compared to the direct sampling method. Note that the noise processes in these figures are the same as those used to compare the predictive powers of physical error metrics in figures 1 and 5. Hence, the employment of importance sampling is key to an honest comparison of the predictive powers of the physical error metrics.

-
- [1] Panos Aliferis and John Preskill. Fault-tolerant quantum computation against biased noise. *Phys. Rev. A*, 78:052331, November 2008.
- [2] Alan Robertson, Christopher Granade, Stephen D. Bartlett, and Steven T. Flammia. Tailored codes for small quantum memories. *Phys. Rev. Applied*, 8:064004, Dec 2017.
- [3] David K. Tuckett, Stephen D. Bartlett, and Steven T. Flammia. Ultrahigh error threshold for surface codes with biased noise. *Phys. Rev. Lett.*, 120:050505, Jan 2018.
- [4] Jérémie Guillaud and Mazyar Mirrahimi. Repetition cat qubits for fault-tolerant quantum computation. *Phys. Rev. X*, 9:041053, December 2019.
- [5] David K Tuckett, Stephen D Bartlett, Steven T Flammia, and Benjamin J Brown. Fault-tolerant thresholds for the surface code in excess of 5% under biased noise. *Phys. Rev. Lett.*, 124(13):130501, 2020.
- [6] J Pablo Bonilla Ataides, David K Tuckett, Stephen D Bartlett, Steven T Flammia, and Benjamin J Brown. The xxxz surface code. *Nat. Commun.*, 12:2172, 2021.
- [7] Panos Aliferis, Daniel Gottesman, and John Preskill. Accuracy threshold for postselected quantum computation. *Quantum Information and Computation*, 8(3&4):0181–0244, 2007.
- [8] Earl T. Campbell, Barbara M. Terhal, and Christophe Vuillot. Roads towards fault-tolerant universal quantum computation. *Nature*, 549(7671):172–179, Sep 2017.
- [9] Easwar Magesan and Paola Cappellaro. Experimentally efficient methods for estimating the performance of quantum measurements. *Phys. Rev. A*, 88:022127, August 2013.
- [10] Pavithran Iyer and David Poulin. A small quantum computer is needed to optimize fault-tolerant protocols. *Quantum Science and Technology*, 3(3):030504, 2018.
- [11] Joel J. Wallman and Joseph Emerson. Noise tailoring for scalable quantum computation via randomized compiling. *Phys. Rev. A*, 94:052325, Nov 2016.
- [12] Alexander Erhard, Joel J. Wallman, Lukas Postler, Michael Meth, Roman Stricker, Esteban A. Martinez, Philipp Schindler, Thomas Monz, Joseph Emerson, and Rainer Blatt. Characterizing large-scale quantum computers via cycle benchmarking. *Nature Communications*, 10(1), Nov 2019.
- [13] Steven T. Flammia and Joel J. Wallman. Efficient estimation of pauli channels. *ACM Transactions on Quantum Computing*, 1(1), December 2020.
- [14] Joel Wallman, Joseph Emerson, Ian Hinks, Egor Ospanov, Dar Dahlen, and Arnaud Carignan-Dugas. Manuscript in preparation. 2021.
- [15] Man-Duen Choi. Completely positive linear maps on complex matrices. *Linear Algebra and its Applications*, 10(3):285–290, June 1975.
- [16] M. A. Nielsen. The entanglement fidelity and quantum error correction. *arXiv:quant-ph/9606012*, 1996.
- [17] Benjamin Schumacher. Sending entanglement through noisy quantum channels. *Phys. Rev. A*, 54:2614–2628, 1996.
- [18] Maxim Raginsky. A fidelity measure for quantum channels. *Physics Letters A*, 290(1):11–18, 2001.
- [19] A Yu Kitaev. Quantum computations: algorithms and error correction. *Russian Mathematical Surveys*, 52(6):1191, 1997.
- [20] A. Yu. Kitaev. *Quantum Error Correction with Imperfect Gates*, pages 181–188. Springer US, Boston, MA, 1997.
- [21] John Watrous. Semidefinite programs for completely bounded norms. *Theory of Computing*, 5:217–238, 2009.
- [22] A.Y. Kitaev, A. Shen, and M.N. Vyalyi. *Classical and Quantum Computation*. Graduate studies in mathematics. American Mathematical Society, 2002.
- [23] Gus Gutoski. On a measure of distance for quantum strategies. *Journal of Mathematical Physics*, 53(3):032202, 2012.
- [24] Alexei Gilchrist, Nathan K. Langford, and Michael A. Nielsen. Distance measures to compare real and ideal quantum processes. *Phys. Rev. A*, 71:062310, 2005.
- [25] E. Knill, D. Leibfried, R. Reichle, J. Britton, R. B. Blakestad, J. D. Jost, C. Langer, R. Ozeri, S. Seidelin, and D. J. Wineland. Randomized benchmarking of quantum gates. *Phys. Rev. A*, 77:012307, Jan 2008.
- [26] Easwar Magesan, J. M. Gambetta, and Joseph Emerson. Scalable and robust randomized benchmarking of quantum processes. *Phys. Rev. Lett.*, 106:180504, May 2011.
- [27] Easwar Magesan, Jay M. Gambetta, and Joseph Emerson. Characterizing quantum gates via randomized benchmarking. *Phys. Rev. A*, 85:042311, Apr 2012.
- [28] D. Aharonov and M. Ben-Or. Fault-tolerant quantum computation with constant error rate. *SIAM Journal on Computing*, 38(4):1207–1282, 2008.
- [29] Krysta M. Svore, David P. Divincenzo, and Barbara M. Terhal. Noise threshold for a fault-tolerant two-dimensional lattice architecture. *Quantum Info. Comput.*, 7(4):297–318, 2007.
- [30] Panos Aliferis and John Preskill. Fibonacci scheme for fault-tolerant quantum computation. *Physical Review A*, 79(1), 2009.
- [31] Barbara M. Terhal and Guido Burkard. Fault-tolerant quantum computation for local non-markovian noise. *Phys. Rev. A*, 71(012336), 2005.
- [32] Donald Bures. An extension of kakutani’s theorem on infinite product measures to the tensor product of semifinite w^* -algebras. *Transactions of the American Mathematical Society*, 135:199–212, 1969.
- [33] A. Uhlmann. The “transition probability” in the state space of a $*$ -algebra. *Reports on Mathematical Physics*, 9(2):273–279, 1976.
- [34] Joel Wallman, Chris Granade, Robin Harper, and

- Steven T Flammia. Estimating the coherence of noise. *New Journal of Physics*, 17(11):113020, 2015.
- [35] Wojciech Roga, Karol Życzkowski, and Fannes Mark. Entropic characterization of quantum operations. *International Journal of Quantum Information*, 09(04):1031–1045, 2011.
- [36] Lin Zhang. Entropy, stochastic matrices, and quantum operations. *Linear and Multilinear Algebra*, 62(3):396–405, 2014.
- [37] Pavithran Iyer. *Une analyse critique de la correction d’erreurs quantiques pour du bruit réaliste*. PhD thesis, Université de Sherbrooke, November 2018.
- [38] Daniel Eric Gottesman. *Stabilizer Codes and Quantum Error Correction*. PhD thesis, California Institute of Technology, May 1997.
- [39] Benjamin Rahn, Andrew C. Doherty, and Hideo Mabuchi. Exact performance of concatenated quantum codes. *Phys. Rev. A.*, 66:032304, 2002.
- [40] Christopher Chamberland, Joel Wallman, Stefanie Beale, and Raymond Laflamme. Hard decoding algorithm for optimizing thresholds under general markovian noise. *Phys. Rev. A*, 95:042332, 2017.
- [41] Emanuel Knill and Raymond Laflamme. Concatenated quantum codes. *arXiv:quant-ph/9608012*, 1996.
- [42] Tomas Jochym-O’Connor and Raymond Laflamme. Using concatenated quantum codes for universal fault-tolerant quantum gates. *Phys. Rev. Lett.*, 112:010505, Jan 2014.
- [43] Min-Hsiu Hsieh and François Le Gall. Np-hardness of decoding quantum error-correction codes. *Phys. Rev. A*, 83(052331), 2011.
- [44] Yu Tomita and Krysta M. Svore. Low-distance surface codes under realistic quantum noise. *Phys. Rev. A*, 90:062320, December 2014.
- [45] David Poulin. Optimal and efficient decoding of concatenated quantum block codes. *Physical Review A*, 74(5), 2006.
- [46] Andrew M. Steane. A tutorial on quantum error correction. In D. L. Shepelyansky G. Casati and P. Zoller, editors, *Quantum Computers, Algorithms and Chaos*, pages 1–32. IOS Press, 2006.
- [47] Robert Raussendorf. Key ideas in quantum error correction. *Philosophical Transactions of the Royal Society A: Mathematical, Physical and Engineering Sciences*, 370(1975):4541–4565, 2012.
- [48] Christopher J. Wood, Jacob D. Biamonte, and David G. Cory. Tensor networks and graphical calculus for open quantum systems. *Quant. Inf. Comp*, 11:0579–0811, 2015.
- [49] Robin Harper, Wenjun Yu, and Steven T. Flammia. Fast estimation of sparse quantum noise. *PRX Quantum*, 2:010322, February 2021.
- [50] Peter D. Johnson, Jonathan Romero, Jonathan Olson, Yudong Cao, and Alán Aspuru-Guzik. Qvector: an algorithm for device-tailored quantum error correction. *arXiv:1711.02249*, 2017.
- [51] Henrik Poulsen Nautrup, Nicolas Delfosse, Vedran Dunjko, Hans J. Briegel, and Nicolai Friis. Optimizing Quantum Error Correction Codes with Reinforcement Learning. *Quantum*, 3:215, December 2019.
- [52] Christopher Chamberland and Pooya Ronagh. Deep neural decoders for near term fault-tolerant experiments. *Quantum Science and Technology*, 3(4):044002, July 2018.
- [53] Milap Sheth, Sara Zafar Jafarzadeh, and Vlad Gheorghiu. Neural ensemble decoding for topological quantum error-correcting codes. *Phys. Rev. A*, 101:032338, March 2020.
- [54] Poulami Das, Christopher A. Pattison, Srilatha Manne, Douglas Carmean, Krysta Svore, Moinuddin Qureshi, and Nicolas Delfosse. A scalable decoder micro-architecture for fault-tolerant quantum computing. *arXiv:2001.06598*, January 2020.
- [55] Akel Hashim, Ravi K. Naik, Alexis Morvan, Jean-Loup Ville, Bradley Mitchell, John Mark Kreikebaum, Marc Davis, Ethan Smith, Costin Iancu, Kevin P. O’Brien, Ian Hincks, Joel J. Wallman, Joseph Emerson, and Irfan Siddiqi. Randomized compiling for scalable quantum computing on a noisy superconducting quantum processor. *arXiv:2010.00215v1*, October 2020.
- [56] K. J. Satzinger, Y. Liu, A. Smith, C. Knapp, et al. Realizing topologically ordered states on a quantum processor. *arXiv:2104.01180*, April 2021.
- [57] Mauricio Gutiérrez and Kenneth R. Brown. Comparison of a quantum error-correction threshold for exact and approximate errors. *Phys. Rev. A*, 91:022335, February 2015.
- [58] D.A. Lidar and T.A. Brun. *Quantum Error Correction*. Cambridge University Press, 2013.
- [59] David P. DiVincenzo and Panos Aliferis. Effective fault-tolerant quantum computation with slow measurements. *Phys. Rev. Lett.*, 98:020501, January 2007.
- [60] Christopher Chamberland, Pavithran Iyer, and David Poulin. Fault-tolerant quantum computing in the Pauli or Clifford frame with slow error diagnostics. *Quantum*, 2:43, 2018.
- [61] J. True Merrill and Kenneth R. Brown. *Progress in Compensating Pulse Sequences for Quantum Computation*, pages 241–294. Advances in Chemical Physics. John Wiley & Sons, Ltd, February 2014.
- [62] Swarnadeep Majumder, Leonardo Andreta de Castro, and Kenneth R. Brown. Real-time calibration with spectator qubits. *npj Quantum Information*, 6(1), Feb 2020.
- [63] Wen Yang, Zhen-Yu Wang, and Ren-Bao Liu. Preserving qubit coherence by dynamical decoupling. *Frontiers of Physics*, 6(1):2–14, Sep 2010.
- [64] Gerardo A. Paz-Silva and D. A. Lidar. Optimally combining dynamical decoupling and quantum error correction. *Scientific Reports*, 3(1), Apr 2013.
- [65] Navin Khaneja, Timo Reiss, Cindie Kehlet, Thomas Schulte-Herbrüggen, and Steffen J. Glaser. Optimal control of coupled spin dynamics: design of nmr pulse sequences by gradient ascent algorithms. *Journal of Magnetic Resonance*, 172(2):296–305, 2005.
- [66] Murphy Yuezhen Niu, Sergio Boixo, Vadim N. Smelyanskiy, and Hartmut Neven. Universal quantum control through deep reinforcement learning. *npj Quantum Information*, 5(1), Apr 2019.
- [67] Daniel Greenbaum and Zachary Dutton. Modeling coherent errors in quantum error correction. *Quantum Science and Technology*, 3(1):015007, 2017.
- [68] Eric Huang, Andrew C. Doherty, and Steven Flammia. Performance of quantum error correction with coherent errors. *Phys. Rev. A*, 99:022313, February 2019.
- [69] Sergey Bravyi, Matthias Englbrecht, Robert König, and Nolan Peard. Correcting coherent errors with surface codes. *npj Quantum Information*, 4(1), Oct 2018.

- [70] These techniques have been discussed for Pauli noise processes in [71, 72].
- [71] Sergey Bravyi and Alexander Vargo. Simulation of rare events in quantum error correction. *Phys. Rev. A*, 88:062308, 2013.
- [72] Colin J Trout, Muyuan Li, Mauricio Gutiérrez, Yukai Wu, Sheng-Tao Wang, Luming Duan, and Kenneth R Brown. Simulating the performance of a distance-3 surface code in a linear ion trap. *New Journal of Physics*, 20(4):043038, 2018.